High-order space and time accuracy for finite volume schemes

Victor Michel-Dansac

Laboratoire de Mathématiques Jean Leray, Université de Nantes

Tuesday, February 23rd, 2016

UNIVERSITÉ DE NANTES

Contents

The equations

2D conservation law with a source term

$$\partial_t W + \operatorname{div}(F(W)) = S(W), \text{ where:}$$

- $W \in \mathbb{R}^n$ is the vector of conserved variables
- $F : \mathbb{R}^n \to \mathcal{M}_{n,2}(\mathbb{R})$ is the physical flux
- $S : \mathbb{R}^n \to \mathbb{R}^n$ is the source term

assume that the homogeneous system $\partial_t W + \operatorname{div}(F(W)) = 0$ is hyperbolic

An example: the shallow-water equations

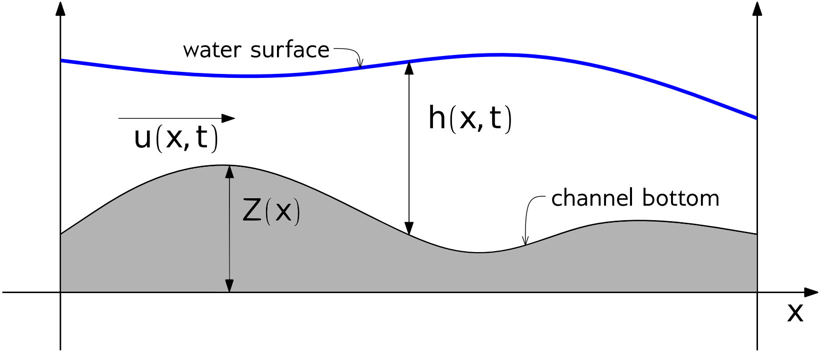

- $h(x,t) \geq 0$: water height
- $u(x,t)$: water velocity
- $Z(x)$: topography (shape of the channel bottom)

An example: the shallow-water equations

2D shallow-water equations with topography

$$
\begin{cases}
\partial_t h + \partial_x(hu) + \partial_y(hv) & = & 0 \\
\partial_t(hu) + \partial_x\left(hu^2 + \frac{1}{2}gh^2\right) + \partial_y\left(huv\right) & = & -gh\partial_x Z \\
\partial_t(hv) + \partial_x\left(huv\right) + \partial_y\left(hv^2 + \frac{1}{2}gh^2\right) & = & -gh\partial_y Z
\end{cases}
$$

$$
W = \begin{pmatrix} h \\ hu \\ hv \end{pmatrix}, \; F(W) = \begin{pmatrix} hu & hv \\ hu^2 + \frac{1}{2}gh^2 & huv \\ huv & hv^2 + \frac{1}{2}gh^2 \end{pmatrix}, \; S(W) = \begin{pmatrix} 0 \\ -gh\partial_x Z \\ -gh\partial_y Z \end{pmatrix}
$$

Objectives and interrogations

Purpose of high-order accuracy

order p: mesh size divided by $2 \Rightarrow$ error divided by 2^p

- have a better solution without refining the mesh
- decrease computational cost

Questions arise!

- how to achieve high-order accuracy?
- what does "better solution" mean?
- what about discontinuous solutions?

First-order vs. High-order

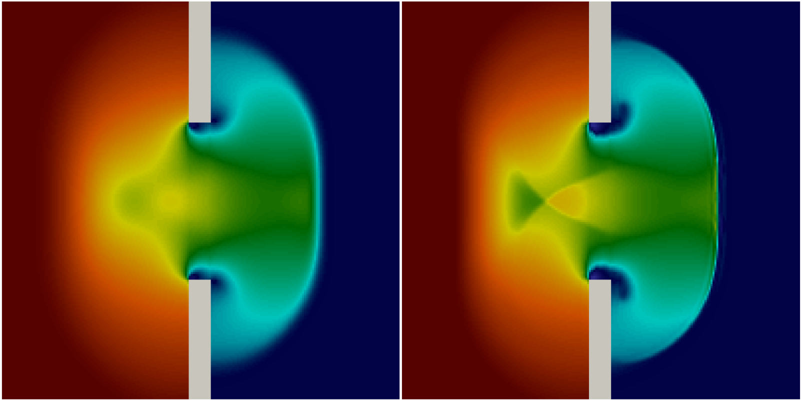

Figure: Partial dam-break, 40000 cells.
Left: first-order scheme. Right: sixth-order scheme.

Finite volume schemes

2D conservation law with a source term

$$\partial_t W + \mathrm{div}(F(W)) = S(W)$$

- $W(x,t) \rightsquigarrow W_i^n$ at time t^n, constant within cell c_i
- $F(W(x,t)) \rightsquigarrow \mathcal{F}_{ij}^n$ at time t^n on the interface between cells c_i and c_j, with $j \in \nu_i$ such that c_j is a direct neighbor of c_i
- $S(W(x,t)) \rightsquigarrow S(W_i^n) =: \mathcal{S}_i^n$ (very naive treatment)

A first-order numerical scheme

$$\frac{W_i^{n+1} - W_i^n}{\Delta t} + \sum_{j \in \nu_i} \frac{|e_{ij}|}{|c_i|} \mathcal{F}_{ij}^n = \mathcal{S}_i^n$$

Second-order extension: 1D illustration

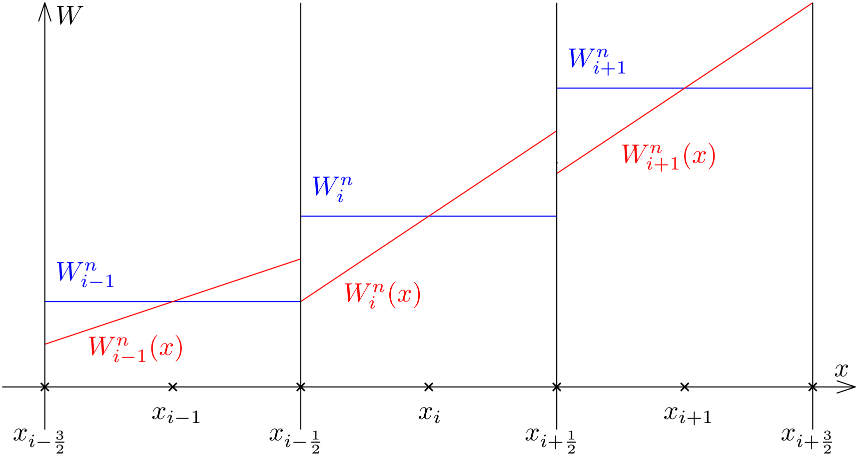

W_i^n constant in cell $c_i \rightsquigarrow W_i^n(x)$ linear in cell c_i

High-order extension: 1D illustration

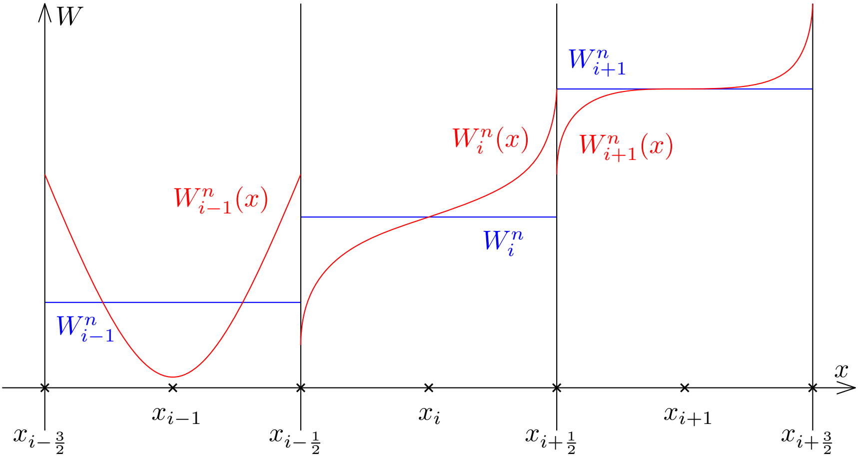

W_i^n constant in cell $c_i \rightsquigarrow W_i^n(x)$ polynomial in cell c_i

Goal of the polynomial reconstruction

given φ a component of W and a cell c_i of center x_i, we know:

- the uniform approximate solution φ_i^n at time t^n
- the degree d of the polynomial reconstruction
- the stencil S_i^d, made of N_d cells

within the cell c_i, we need:

- a polynomial reconstruction $\hat{\varphi}_i^n(x)$ at time t^n:
  $\hat{\varphi}_i^n(x)$ is a degree d polynomial
- the conservation property: $\dfrac{1}{|c_i|} \displaystyle\int_{c_i} \hat{\varphi}_i^n(x) dx = \varphi_i^n$

Construction of the polynomial in 1D

$$\text{set } \hat{\varphi}_i^n(x) = \sum_{k=0}^{d} \left[\alpha_i^k (x - x_i)^k + \beta_i^k\right], \text{ recall } \frac{1}{|c_i|} \int_{c_i} \hat{\varphi}_i^n(x) dx = \varphi_i^n$$

- valid reconstruction for $d = 0 \rightsquigarrow \alpha_i^0 + \beta_i^0 = \varphi_i^n$
- $d > 0 \rightsquigarrow \forall k \in [\![1, d]\!],\ \beta_i^k = -\dfrac{\alpha_i^k}{|c_i|} \displaystyle\int_{c_i} (x - x_i)^k dx$

$$\text{therefore } \hat{\varphi}_i^n(x) = \varphi_i^n + \sum_{k=1}^{d} \alpha_i^k \left[(x - x_i)^k - \frac{1}{|c_i|} \int_{c_i} (x - x_i)^k dx\right]$$

what is left to do:
determine the polynomial coefficients α_i^k using the stencil S_i^d

Construction of the polynomial in 2D

from the 1D formula and $M_i^k = \dfrac{1}{|c_i|}\displaystyle\int_{c_i}(x - x_i)^k dx$, we get:

$$\hat{\varphi}_i^n(x) = \varphi_i^n + \sum_{|k|=1}^{d} \alpha_i^k \left[(x - x_i)^k - M_i^k\right]$$

the α_i^k are chosen to minimize the least squares error E_i between the reconstruction and φ_j^n, for all j in the stencil S_i^d:

$$E_i(\alpha_i) = \frac{1}{2}\sum_{j \in S_i^d}\left[\frac{1}{|c_j|}\int_{c_j}\hat{\varphi}_i^n(x) - \varphi_j^n\right]^2$$

Construction of the polynomial in 2D

$$E_i(\alpha_i) = \frac{1}{2} \sum_{j \in S_i^d} \left[\frac{1}{|c_j|} \int_{c_j} \hat{\varphi}_i^n(x) - \varphi_j^n \right]^2$$
$$= \frac{1}{2} \|X_i \alpha_i - \Phi_i\|^2$$

overdetermined system $\Leftarrow \#S_i^d \geq \dfrac{(d+1)(d+2)}{2} - 1$

α_i minimizes $E_i(\alpha_i) \Longleftrightarrow {}^t X_i X_i \alpha_i = {}^t X_i \Phi_i$ (normal equation)

if ${}^t X_i X_i$ is invertible (depends on the choice of the stencil), then

$$\alpha_i \text{ minimizes } E_i(\alpha_i) \Longleftrightarrow \alpha_i = \left({}^t X_i X_i\right)^{-1} {}^t X_i \Phi_i$$

Summary

$$\hat{\varphi}_i^n(x) = \varphi_i^n + \sum_{|k|=1}^{d} \alpha_i^k \left[(x - x_i)^k - M_i^k \right]$$

with $\alpha_i = \left({}^t X_i X_i \right)^{-1} {}^t X_i \Phi_i$, and where we have defined:

- $M_i^k = \dfrac{1}{|c_i|} \displaystyle\int_{c_i} (x - x_i)^k dx$
- $\Phi_i = \left(\varphi_j^n - \varphi_i^n \right)_{j \in S_i^d}$
- $X_i = \left[\dfrac{1}{|c_j|} \displaystyle\int_{c_j} (x - x_i)^k dx - \dfrac{1}{|c_i|} \displaystyle\int_{c_i} (x - x_i)^k dx \right]_{k \in [\![1,d]\!],\, j \in S_i^d}$

Mesh notations

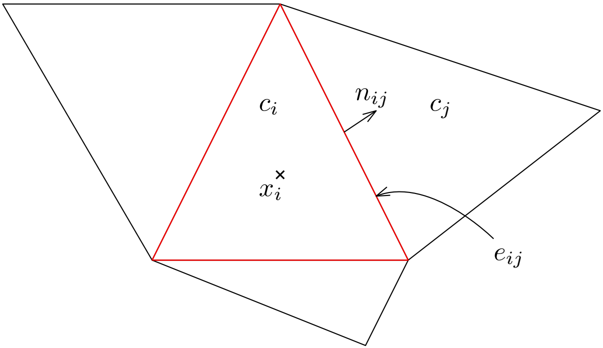

Resources at our disposal

Build a high-order scheme for $\partial_t W + \operatorname{div}(F(W)) = S(W)$, using:

1. the polynomial reconstruction $\widehat{W}_i^n(x)$;
2. $F(W)\cdot n_{ij} \simeq \mathcal{F}\left(\widehat{W}_i^n(x), \widehat{W}_j^n(x); n_{ij}\right)$, with $\mathcal{F}$ numerical flux;
3. (ξ_r, x_r), a quadrature on e_{ij}: $\dfrac{1}{|e_{ij}|}\displaystyle\int_{e_{ij}} f(x)dx \simeq \sum_{r=0}^{R} \xi_r f(x_r)$;
4. $W(x,t) \simeq \widehat{W}_i^n(x)$, for $(x,t) \in c_i \times [t^n, t^{n+1})$;
5. (η_q, x_q), a quadrature on c_i: $\dfrac{1}{|c_i|}\displaystyle\int_{c_i} f(x)dx \simeq \sum_{q=0}^{Q} \eta_q f(x_q)$;
6. the conservation property $W_i^n = \dfrac{1}{|c_i|}\displaystyle\int_{c_i} \widehat{W}_i^n(x)dx$.

The high-order scheme

First-order numerical scheme

$$W_i^{n+1} = W_i^n - \Delta t \sum_{j \in \nu_i} \frac{|e_{ij}|}{|c_i|} \mathcal{F}_{ij}^n + \Delta t \, \mathcal{S}_i^n$$

High-order numerical scheme

$$W_i^{n+1} = W_i^n - \Delta t \sum_{j \in \nu_i} \frac{|e_{ij}|}{|c_i|} \sum_{r=0}^{R} \xi_r \mathcal{F}_{ij,r}^n + \Delta t \sum_{q=0}^{Q} \eta_q \mathcal{S}_{i,q}^n$$

Runge-Kutta methods

rewrite the high-order numerical scheme as $W^{n+1} = \mathcal{H}(W^n)$

Goal of the Runge-Kutta method

Obtain high-order time accuracy from a scheme that is first-order accurate in time.

A second-order example: Heun's method

$$\begin{aligned} W^{n+\frac{1}{2}} &= \mathcal{H}(W^n) \\ W^{n+1} &= \frac{1}{2}\left[W^n + \mathcal{H}\left(W^{n+\frac{1}{2}}\right)\right] \end{aligned}$$

Strong-Stability Preserving Runge-Kutta methods

goal of a SSPRK method: if $\mathcal{H}$ is robust in some sense, then the high-order time discretization SSPRK is also robust

Robustness examples

1D definition: total variation $\mathrm{TV}(W^n) = \sum_i \left(W_{i+1}^n - W_i^n\right)$

- non-negativity preservation: $\phi_i^n \geq 0 \Rightarrow \phi_i^{n+1} \geq 0$
- total variation diminishing: $\mathrm{TV}(W^{n+1}) \leq \mathrm{TV}(W^n)$
- total variation bounded: $\mathrm{TV}(W^n) \leq M \Rightarrow \mathrm{TV}(W^{n+1}) \leq M$
- entropy preservation

Strong-Stability Preserving Runge-Kutta methods

SSPRK3 method

$$W^{n+\frac{1}{3}} = \mathcal{H}(W^n)$$

$$W^{n+\frac{2}{3}} = \mathcal{H}(W^{n+\frac{1}{3}})$$

$$W^{n+1} = \frac{1}{3}\left[W^n + 2\mathcal{H}\left(\frac{3W^n + W^{n+\frac{2}{3}}}{4}\right)\right]$$

SSPRK3 is third-order accurate in time: to get time accuracy of order p, we set, instead of Δt,

$$\Delta t = \Delta t^{\frac{\max(p,3)}{3}}$$

The 2D shallow-water equations with topography and friction

$$\begin{cases} \partial_t h + \partial_x(hu) + \partial_y(hv) & = & 0 \\ \partial_t(hu) + \partial_x \left(hu^2 + \dfrac{1}{2} g h^2 \right) + \partial_y (huv) & = & -gh\partial_x Z - ku\sqrt{u^2+v^2} h^{-1/3} \\ \partial_t(hv) + \partial_x (huv) + \partial_y \left(hv^2 + \dfrac{1}{2} g h^2 \right) & = & -gh\partial_y Z - kv\sqrt{u^2+v^2} h^{-1/3} \end{cases}$$

- robustness: we must have $h \geq 0$
- steady state solutions: $\partial_t h = \partial_t(hu) = \partial_t(hv) = 0$

Order of accuracy assessment

$e_\delta = C\delta^p$, with p the order, e_δ the error and δ the mesh size
$\rightsquigarrow \ln(e_\delta) = \ln C + p \ln \delta$, line of slope p

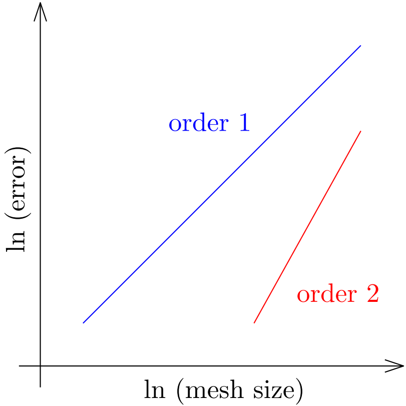

$$p = \frac{\ln(e_\delta) - \ln(e_{\delta'})}{\ln \delta - \ln \delta'} : \text{ if } \delta' = 2\delta, \text{ then } p = \frac{\ln(e_\delta) - \ln(e_{\delta'})}{\ln 2}$$

The steady vortex

steady state without friction, where W depends only on $x^2 + y^2$

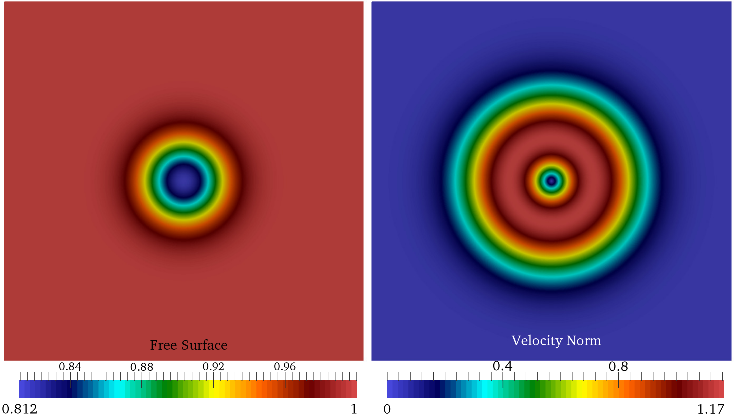

Figure: Left panel: free surface. Right panel: velocity norm (the vortex flows clockwise). Space domain: $[-3, 3]^2$.

Order of accuracy assessment: steady vortex

N	L^1		L^2		L^∞	
1024	6.37e-03	—	1.61e-02	—	1.19e-01	—
4096	4.31e-03	0.56	1.08e-02	0.58	7.88e-02	0.59
16384	2.58e-03	0.74	6.43e-03	0.75	4.58e-02	0.78

Table: First-order scheme, height error.

N	L^1		L^2		L^∞	
900	2.04E-05	—	5.22E-05	—	7.84E-04	—
3600	3.07E-07	6.05	6.88E-07	6.25	9.94E-06	6.30
14400	3.93E-09	6.29	5.82E-09	6.88	5.53E-08	7.49

Table: Sixth-order scheme, height error.

Radial friction experiment

steady state with friction, with a singularity at the origin

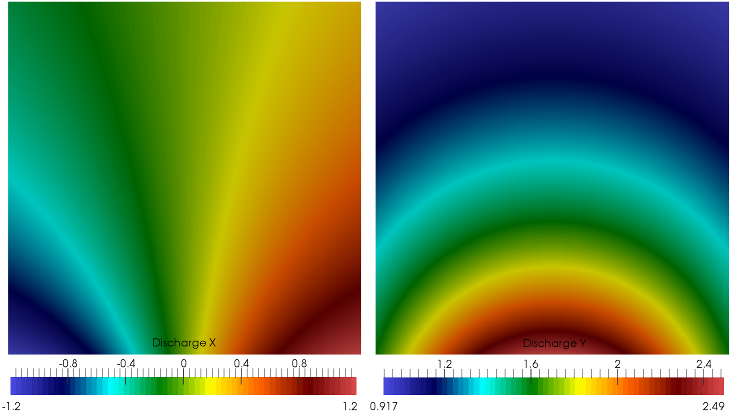

Figure: Left panel: discharge in the x-direction. Right panel: discharge in the y-direction. Space domain: $[-0.3, 0.3] \times [0.4, 1]$.

Order of accuracy assessment: radial friction experiment

N	h		q_x		q_y	
900	2.37e-08	—	8.00e-08	—	1.12e-07	—
3600	3.77e-10	5.98	1.28e-09	5.96	1.82e-09	5.94
14400	5.89e-12	6.00	1.99e-11	6.01	2.91e-11	5.96
57600	1.24e-14	8.89	2.06e-13	6.60	1.20e-13	7.92

Table: L^1 errors, sixth-order scheme.

N	h		q_x		q_y	
900	1.04e-07	—	5.20e-07	—	5.57e-07	—
3600	1.80e-09	5.86	8.15e-09	6.00	1.02e-08	5.77
14400	3.38e-11	5.73	1.25e-10	6.02	1.71e-10	5.89
57600	8.33e-13	5.34	2.26e-12	5.79	2.59e-12	6.05

Table: L^∞ errors, sixth-order scheme.

1D dam-break

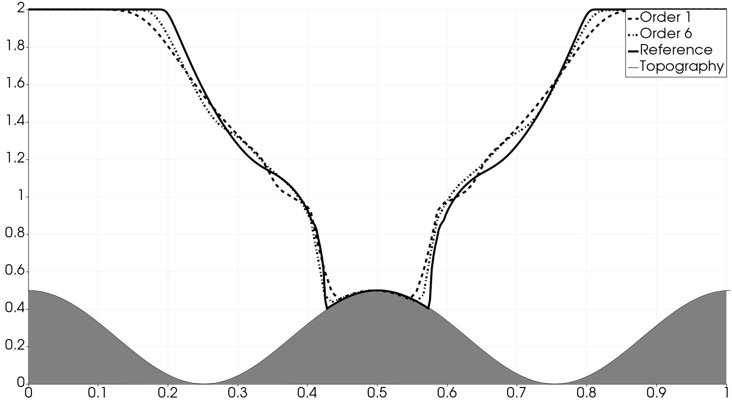

Figure: Free surface for the dam-break over a dry sinusoidal bottom: reference solution and results of first-order and sixth-order schemes. The gray area represents the topography. 100 cells were used.

2D partial dam-break

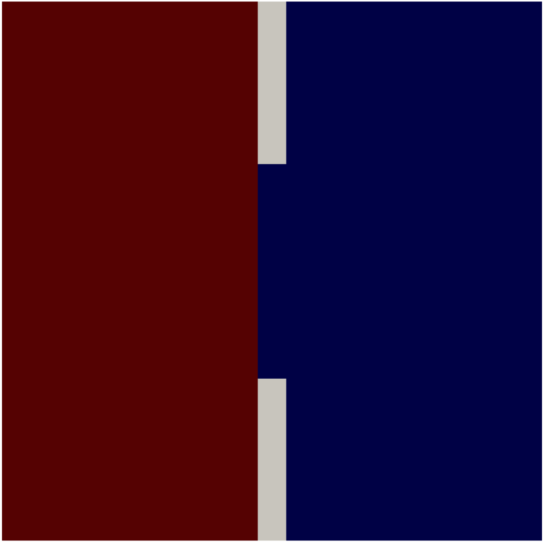

Simulation of the 2011 Japan tsunami

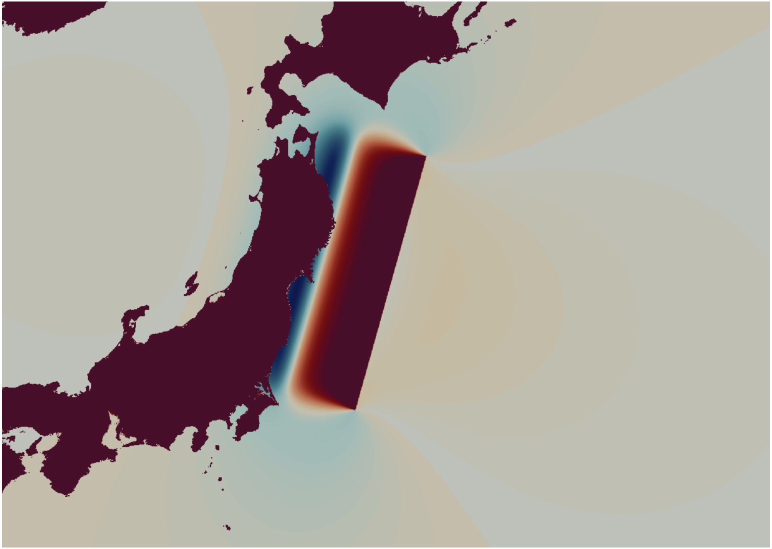

Conclusion

- polynomial reconstruction of order d using a relevant stencil
- high-order space accuracy: integration of the equations
- high-order time accuracy: SSPRK methods

Going further

- the polynomial reconstruction may produce oscillations or non-physical values (for instance $h < 0$): use the MOOD method to lower the reconstruction degree
- a steady state is modified by the reconstruction: a first-order well-balanced scheme will not stay well-balanced when the high-order strategy is applied

Thank you for your attention!